Spin-Parity Analysis of the A_3†

G. Ascoli, D. V. Brockway,* L. Eisenstein, J. D. Hansen,‡ M. L. Ioffredo,§ and U. E. Kruse
Department of Physics, University of Illinois at Champaign – Urbana, Urbana, Illinois 61801

and

T. F. Johnston, A. W. Key, J. D. Prentice, and T. S. Yoon
Physics Department, University of Toronto, Toronto, Ontario, Canada

and

C. Caso and G. Tomasini
Istituto di Fisica dell'Università, Genova, Italy
and Istituto Nazionale di Fisica Nucleare, Sezione di Genova, Genova, Italy

and

P. von Handel and P. Schilling
Deutsches Elektronen Synchrotron, Hamburg, Germany
and II. Institut für Experimentalphysik, Universität Hamburg, Hamburg, Germany

and

G. Costa and S. Ratti
Istituto di Scienze Fisiche dell'Università, Milano, Italy
and Istituto Nazionale di Fisica Nucleare, Sezione di Milano, Milano, Italy

and

L. Mosca
Département de Physique des Particules Elémentaires, Centre d'Etudes Nucléaires de Saclay, Gif-sur-Yvette, France

and

W. C. Harrison,‖ D. Heyda, W. H. Johnson, Jr., J. K. Kim, M. E. Law, J. E. Mueller,**
B. M. Salzberg,†† and L. K. Sisterson
Lyman Laboratory of Physics, Harvard University, Cambridge, Massachusetts 02138

and

H. Grässler
III. Physikalisches Institut der Technischen Hochschule, Aachen, Germany

and

W. D. Nowak
Institut für Hochenergiephysik der Deutschen Akademie der Wissenschaften zu Berlin, Zeuthen, D.D.R.

and

M. Rost
Physikalisches Institut der Universität, Bonn, Germany

and

G. T. Jones and W. Kittel
CERN, European Organization for Nuclear Research, Geneva, Switzerland

and

S. Brandt
Institut für Hochenergiephysik, Heidelberg, Germany

and

P. H. Smith,‡‡ W. D. Shephard, N. N. Biswas, N. M. Cason, V. P. Kenney,§§ and W. B. Madden‖‖
Physics Department, Notre Dame University, Notre Dame, Indiana 46556

and

A. R. Erwin, R. Morse,*** B. Y. Oh,††† W. Robertson,‡‡‡ and W. D. Walker‡‡‡
Physics Department, University of Wisconsin, Madison, Wisconsin 53706
(Received 17 July 1972)

A partial-wave analysis of the charged three-pion system in the reaction $\pi^- p \to p\pi^+\pi^-\pi^-$ for incident π^- momenta from 5 to 25 GeV/c shows the existence of a broad enhancement ($\sim$ 300 MeV) in the $J^P = 2^- f\pi$ (S-wave) state in the region of the $A_3(1650)$. No other state ($J \leq 4$) shows structure in this region. Upper bounds for $\rho\pi$ and $\epsilon\pi$ decay modes of the A_3 are given. The interference of the $2^- f\pi$ (S-wave) amplitude with other amplitudes has been observed. The mass variation of the phase of the $2^- f\pi$ (S-wave) amplitude measured with respect to the phases of other amplitudes does not show the behavior expected for the relative phase between resonant and nonresonant amplitudes. Results are given on the polarization and momentum-transfer dependence of the A_3 and on the A_3 production cross section as a function of incident π^- momentum.

I. INTRODUCTION AND SUMMARY

The A_3 is an enhancement at $M \sim 1.65$ GeV observed in the three-pion state produced in the reactions $\pi^\pm p \to \pi^\pm\pi^+\pi^- p$.[1] Estimates of the A_3 width have ranged from 0.05 to 0.4 GeV. A substantial fraction of the enhancement is believed to occur in the $f^0\pi$ channel,[2-4] but enhancements in other channels – in particular in the "direct" 3π channel – have also been reported.[2,5] The proximity of the A_3 to the $f^0\pi$ threshold has led to the guess that the A_3 may have spin-parity $J^P = 2^-$ and also to the speculation that it may be a Deck[6] rather than a resonance phenomenon. Previous studies[2,4] have not led to an unambiguous determination of the spin and parity of the A_3. Recently the analysis of an 11.7-GeV π^+ experiment has led Caso *et al.*[7] to conclude that the $f^0\pi$ contribution to the A_3 enhancements in other spin-parity states (in particular in the state $J^P = 0^-$, decaying into $\epsilon^0\pi$) were also found in this study.

In this paper we present a detailed account of an analysis of the 3π system observed in a series of $\pi^- p \to \pi^-\pi^-\pi^+ p$ experiments at incident momenta from 5 to 25 GeV/c. By a method[8] based on fitting the complete "decay" distribution (Dalitz and angle variables) of the 3π system we have sorted out the contributions of different spin-parity states (for $J \leq 4$) and of different decay modes ($\epsilon^0\pi^-$, $\rho^0\pi^-$, $f^0\pi^-$, and – to some extent – "3π") in the A_3 region ($M_{3\pi} = 1.5$–1.8 GeV) and considered in detail the $M_{3\pi}$ dependence over a wider region.

Our results concerning the A_3 phenomenon are:

(1) The only J^P state showing an enhancement in the A_3 region is $J^P = 2^-$.

(2) The only channel showing an enhancement in the A_3 region is in the $f^0\pi$ channel, with orbital angular momentum $l = 0$. No enhancement is seen in the channels $\epsilon^0\pi$, $\rho^0\pi$, or 3π either for $J^P = 2^-$ or any other J^P state.

(3) The A_3 enhancement, $J^P = 2^-(S \to f^0\pi)$,[9] is well fitted by a Breit-Wigner shape with $M = 1.66 \pm 0.01$ GeV and $\Gamma = 0.27 \pm 0.06$ GeV.

(4) The interference term between the production amplitudes for $2^-(S \to f^0\pi)$ and $2^-(P \to \rho^0\pi)$ has been observed. Although the S wave peaks in the A_3 region and the P wave does not, the relative phase does not vary significantly with $M_{3\pi}$.

(5) The interference terms between the production amplitude for $2^-(S \to f^0\pi)$ and the amplitude for the states 0^-, 1^+, and 3^+ have also been observed. Again, although only the $2^-(S)$ amplitude peaks in A_3 region, no variation of the relative phases with $M_{3\pi}$ is observed.

(6) The differential cross section $d\sigma/dt'$ for $A_3(2^-S)$ production decreases exponentially with t'.[10] The observed exponent is 7.7 ± 0.8 GeV^{-2}.

(7) The polarization of the A_3 has been observed. In the t-channel frame, the most important magnetic substate is $|2^-0\rangle$, with a small but measurable contribution in the substate $|2^-1\rangle - |2^-{-1}\rangle$. The polarization, in the t-channel frame, does not depend significantly on t'.

(8) In the range 11–25 GeV the dependence of the $\pi^- p \to A_3^- p$ cross section on laboratory momentum is consistent with a power-law dependence. If such a power-law dependence is assumed the power is -0.8 ± 0.3 and the cross section for production of A_3^- (more precisely for production of $J^P = 2^- \to f^0\pi \to \pi^+\pi^-\pi^-$, with $M_{3\pi} = 1.5$–1.8 GeV and $t' < 0.7$ GeV^2) in the reaction $\pi^- p \to A_3^- p$ is 35 ± 4 μb at 16 GeV.

TABLE I. List of experiments with the number of $\pi^- p \to p\pi^+\pi^-\pi^-$ events at each momentum.

Momentum (GeV/c)	No. of events	No. of events in A_3 region [a]	Group
5	26251	1073	University of Illinois
7	5483	391	Toronto-Wisconsin
7.5	10904	707	University of Illinois
11	3403	403	Genova-Hamburg-Milano-Saclay
13	2150	233	Harvard University
16	5186	584	Aachen-Berlin-Bonn-CERN-Heidelberg
18.5	4799	548	Notre Dame University
20	3680	401	Harvard University
25	2119	253	University of Wisconsin

[a] This region is defined by $1.5 < M_{3\pi} < 1.8$ GeV, $t' < 0.7$ GeV^2. For 11–25-GeV/c experiments events with $1.16 < M_{p\pi^+} < 1.32$ GeV are excluded. For 5–7.5-GeV/c experiments events with $M_{p\pi^+} < 1.4$ GeV or $1.16 < M_{p\pi^-} < 1.32$ GeV are excluded.

II. EXPERIMENTAL DATA

The data discussed in this paper come from a study of the reaction $\pi^- p \to p\pi^-\pi^-\pi^+$ in a series of hydrogen bubble-chamber exposures at incident momenta from 5 to 25 GeV/c (see Table I). In this section we survey the main features of the data. Because of the problems caused by the presence of strong Δ^{++} and Δ^0 signals at the lower incident momenta, we present separately the results of the low-energy ($p_{\text{lab}} = 5, 7, 7.5$ GeV/c) and of the high-energy ($p_{\text{lab}} = 11, 13, 16, 18.5, 20, 25$ GeV/c) experiments.

Figures 1 and 2 show the 3π mass spectra for all events and (shaded) for events after the indicated cuts on t'[11] and on $p\pi$ masses. In the high-energy data two enhancements are clearly seen. The enhancement at $M_{3\pi} = 1.0$–1.4 GeV is due to A_1 and A_2 production. The enhancement centered at $M_{3\pi} \sim 1.65$ GeV, the A_3, is the subject of this paper. Similar enhancements are seen in the low-energy data; however, the A_3 signal is less prominent, particularly after the cuts (shaded histograms). Figure 3 shows the 3π mass spectra (with the same t' and Δ cuts as the shaded histograms in Figs. 1 and 2) for events with at least one $\pi^+\pi^-$ combination in the f^0 mass region (1.14–1.36 GeV). Clear A_3 peaks are seen, which

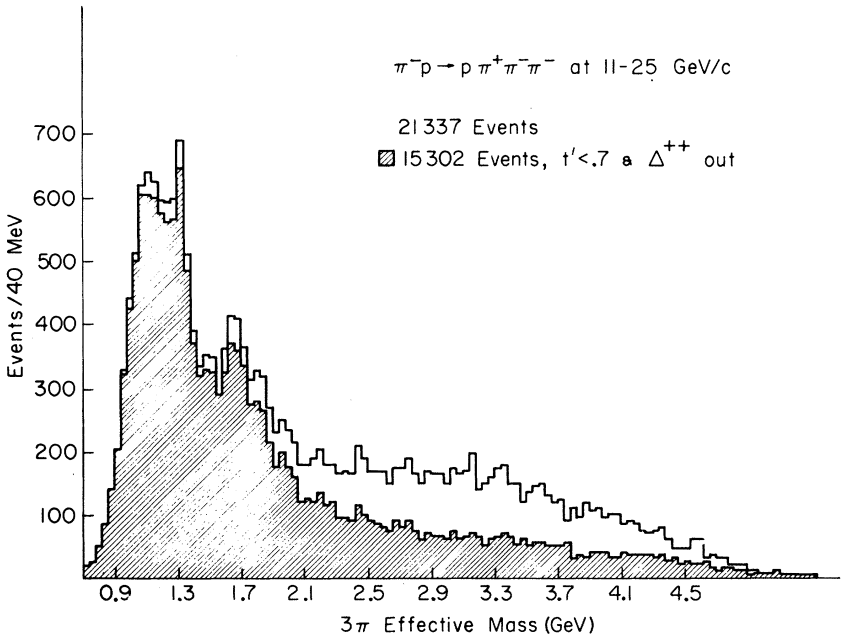

FIG. 1. $\pi^+\pi^-\pi^-$ mass spectrum for the 11–25-GeV/c data. The shaded histogram is for $t' < 0.7$ GeV^2, $M_{p\pi^+} = 1.16$–1.32 GeV out.

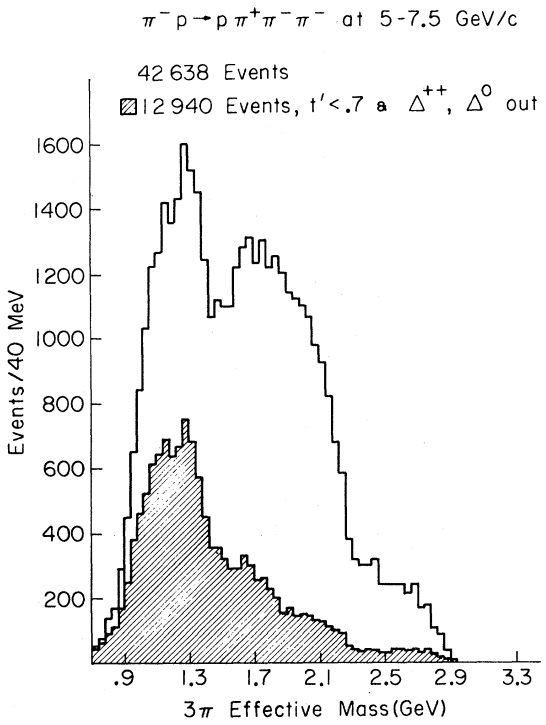

FIG. 2. $\pi^+\pi^-\pi^-$ mass spectrum for the 5–7.5-GeV/c data. The shaded histogram is for $t' < 0.7$ GeV^2, $M_{p\pi^+} < 1.4$ GeV out, $M_{p\pi^-} = 1.16$–1.32 GeV out.

survive after events with a $\pi^+\pi^-$ combination in the ρ^0 mass region (0.665–0.865 GeV) are removed. Comparison with the unselected spectra (shaded histograms, Figs. 1 and 2) makes it plausible that a substantial part, perhaps all, of the A_3 enhancements are due to $f^0\pi^-$ events. The width of the $f^0\pi^-$ peaks is about 0.3 GeV with no evidence of finer structure.

A. Δ^{++} and Δ^0 Production

Our aim is to study the $\pi^+\pi^-\pi^-$ system in the neighborhood of the A_3. The presence of a strong interaction between the proton and any of the π's in the final state will certainly complicate the analysis. Figures 4 and 5 show the $p\pi^+$ and $p\pi^-$ mass spectra for events in the A_3 region ($M_{3\pi}$ = 1.5–1.8 GeV, $t' < 0.7$ GeV^2). In the high-energy data there is a modest $\Delta^{++}(1236)$ signal and no apparent structure in the $p\pi^-$ spectrum. To simplify the analysis we therefore remove events with $M(p\pi^+)$ between 1.16 and 1.32 GeV. In the analysis of the data we can and do take into account the effect of such a Δ^{++} cut. We have further verified that the results, after correcting for the cuts, are independent of the width of the Δ^{++} cut (and of the presence or absence of a Δ^0

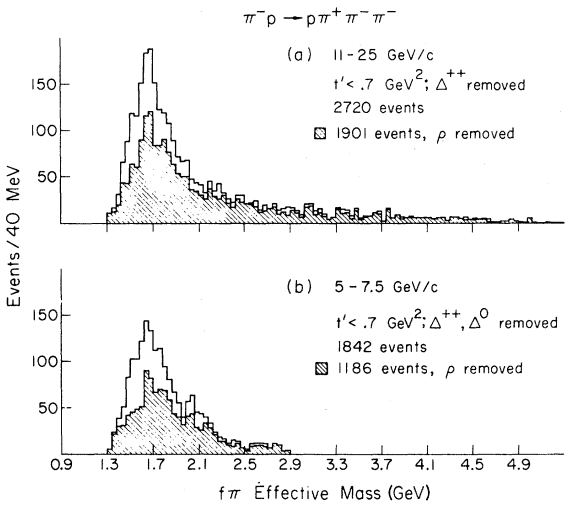

FIG. 3. 3-π mass spectra for events with at least one $\pi^+\pi^-$ mass in f^0 (1.14–1.36 GeV). In the shaded histograms events with a $\pi^+\pi^-$ mass in ρ^0 (0.665–0.865 GeV) are removed. (a) 11–25-GeV/c data: $t' < 0.7$ GeV^2, $M_{p\pi^+} = 1.16$–1.32 GeV out; (b) 5–7.5-GeV/c data: $t' < 0.7$ GeV^2, $M_{p\pi^+} < 1.4$ GeV out, $M_{p\pi^-} = 1.16$–1.32 GeV out.

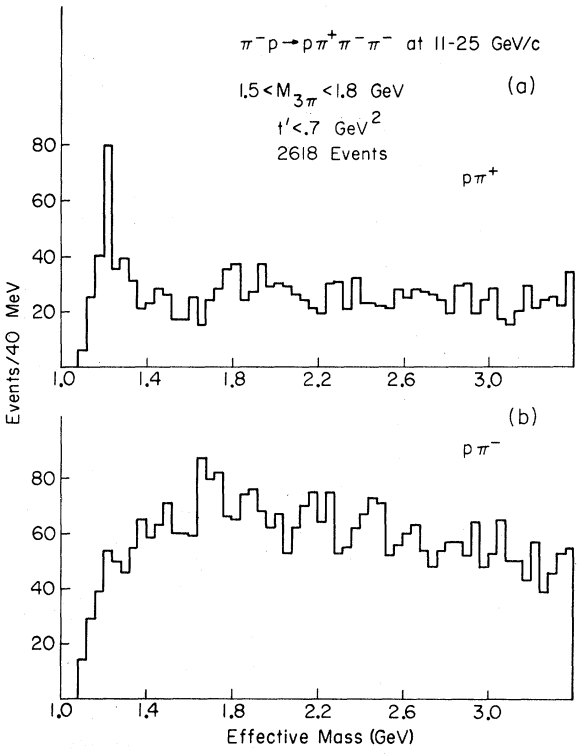

FIG. 4. (a) $p\pi^+$ mass spectrum for A_3-region ($M_{3\pi}$ = 1.5–1.8 GeV, $t' < 0.7$ GeV^2) events in 11–25-GeV/c data; (b) $p\pi^-$ mass spectrum (2 combinations per event) for the same events.

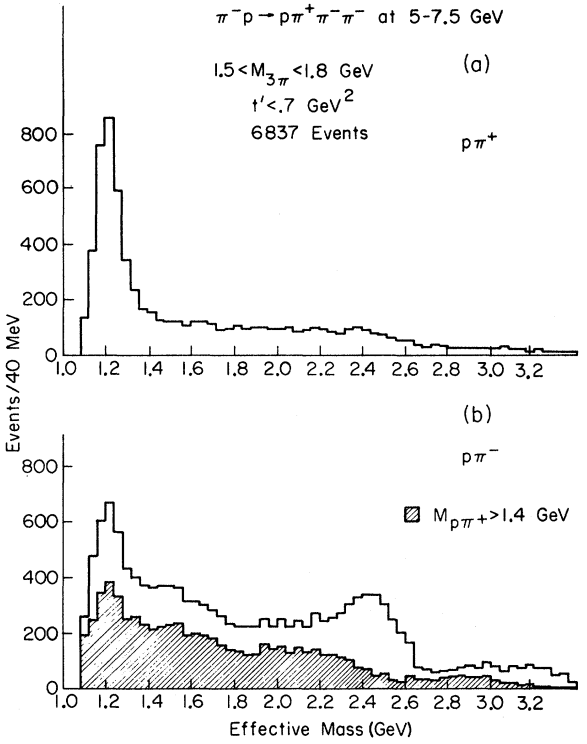

FIG. 5. (a) $p\pi^+$ mass spectrum for A_3-region ($M_{3\pi}$ = 1.5–1.8 GeV, $t' < 0.7$ GeV^2) events in 5–7.5 GeV/c data; (b) $p\pi^-$ mass spectrum (2 combinations per event) for the same events, shaded histogram: $M_{p\pi^+} < 1.4$ GeV out.

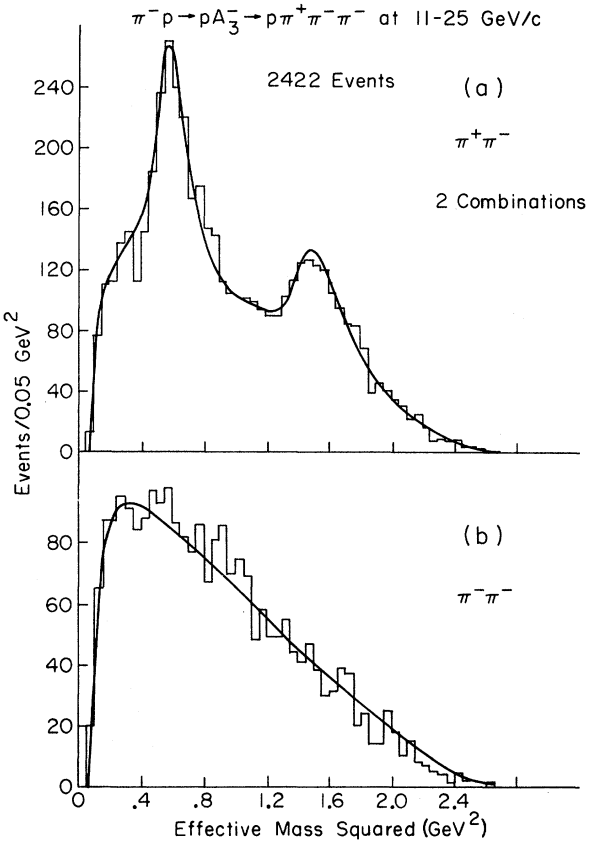

FIG. 6. Dalitz-plot projections in A_3 region of the 11–25-GeV/c data (see Ref. 12).

cut).

The situation is quite different for the low-energy data. Figure 5 shows a very strong Δ^{++} signal and a significant Δ^0 signal. To remove these signals from the data we have chosen to remove all events with $M(p\pi^+)$ below 1.4 GeV or $M(p\pi^-)$ between 1.16 and 1.32 GeV. As may be seen by referring to Fig. 2 these are drastic cuts. About 70% of the events in the A_3 mass region are removed and the (calculated) loss of "true A_3" events (state $J^P M = 2^-0$, decaying into $f^0\pi^-$) is about 40%. With such a drastic mutilation of the data it is not surprising that the results of the analysis are not completely independent of the choice of width for these cuts. The main conclusions presented in this paper are however independent of the precise choice of cuts applied to the low-energy data.

B. Decay Distributions in the A_3 Region

The detailed analysis discussed in subsequent sections is based on the distribution of events in 5-dimensional space (2 Dalitz-plot variables and 3 Euler angles). In this section we present various projections of the decay distribution. The data are shown in Figs. 6–12 for events in the A_3 region.[12] The curves shown are the results of the fits described in Sec. III and take into account the effect of the cuts.

Figures 6–9 give information about the Dalitz-plot distribution of the events. The Dalitz-plot projections (Figs. 6 and 7) show that strong ρ^0 and f^0 bands are present. From the results of the fit (or by analysis of the Dalitz plot alone)[13] one finds contributions (in the high-energy data) of about 35% from $f^0\pi^-$, 40% from $\rho^0\pi^-$, and 25% from $\epsilon^0\pi^-$ (and 3π). Figures 8 and 9 show the density of events along the f^0 and ρ^0 bands. The only obvious features are those due to the crossing of the other ρ^0 and f^0 bands.

We look next at the decay angular distributions: Figs. 10 and 11 give the distribution in the Euler angles θ, ϕ, γ, and Fig. 12 the distributions in $\hat{\pi}_{\text{in}} \cdot \hat{f}^0$ and $\hat{\pi}_{\text{in}} \cdot \hat{\rho}^0$. As discussed in Sec. V, the angular distributions are independent of t when t-channel axes (Gottfried-Jackson axes) are used. Therefore the angular distributions shown in Figs. 10–12 refer to t-channel axes.[14] The angles θ and ϕ are the polar and azimuthal angles of the

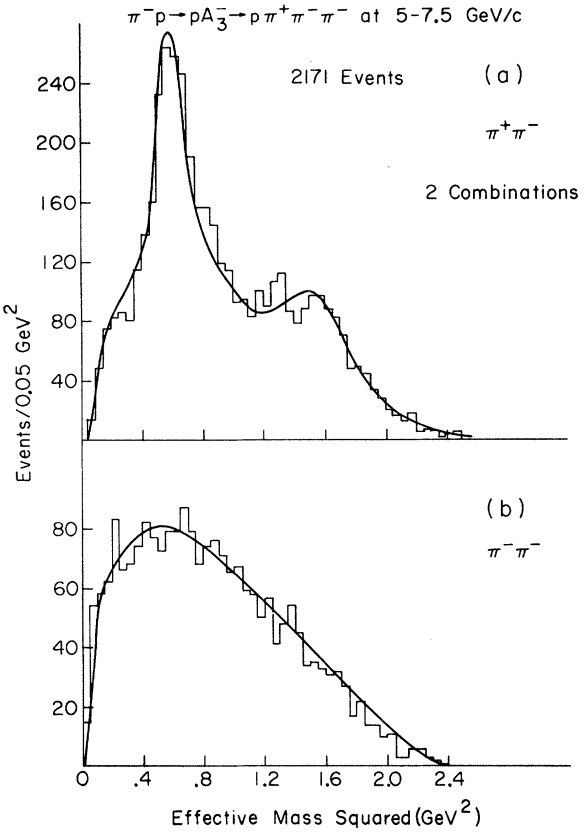

FIG. 7. Dalitz-plot projections in A_3 region of the 5–7.5-GeV/c data (see Ref. 12).

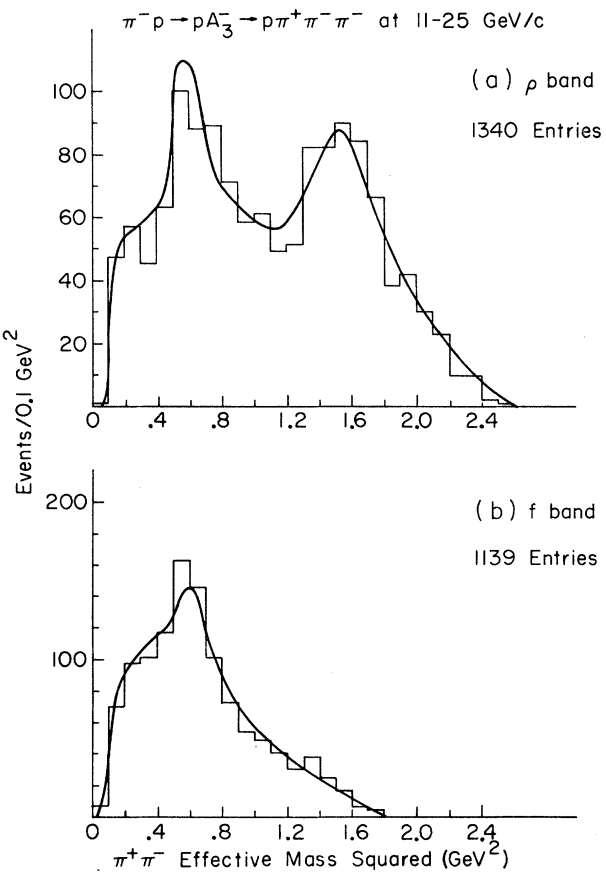

FIG. 8. (a) ρ^0 band (0.665–0.865 GeV); (b) f^0 band (1.41–1.36 GeV) projections for A_3 region of the 11–25-GeV/c data (see Ref. 12).

π^+; γ is the angle between the 3π plane and the plane containing $\hat{z}$ and $\hat{\pi}^+$.[15]

We note that

(a) the distributions for the low-energy and the high-energy data are quite similar, the differences being mostly a consequence of the Δ^{++} cuts;

(b) the distribution in $\cos\theta$ for $f^0\pi^-$ events is close to $|Y_{20}|^2$ apart from a moderate asymmetry[16];

(c) the ϕ distribution for $f^0\pi^-$ (as well as for all events) is nearly uniform[16];

(d) the distribution in $\hat{\pi}_{\text{in}}^- \cdot \hat{f}^0$ (Fig. 12) is predominantly S wave (about 75–80% for the high-energy data).

(b), (c), and (d) indicate that the $f^0\pi^-$ in the A_3 region is an S-wave decay of a $J^P = 2^-$, $J_z = 0$ state.

There are indications also that the ρ-π system is quite complicated in the A_3 region.

(e) The γ distribution for all events has a sharp peak (in the high-energy data) indicating that angular momenta up to at least $J = 4$ may be required to fit the data.

III. PARTIAL-WAVE ANALYSIS

A. Method

The method used to decompose the $\pi^+\pi^-\pi^-$ data into contributions from different partial waves is to make a maximum-likelihood fit to the distribution of events in the 5-dimensional decay space. At fixed incident momentum, fixed momentum transfer, and fixed 3π mass the coordinates used to describe the decay configuration of each event are the Dalitz plot coordinates $[s_1 = M^2(\pi^+\pi_2^-), s_2 = M^2(\pi^+\pi_1^-)]$ and a set of three Euler angles. Each event is assigned a probability, P, given by

$$P = \sum_{ab} \rho_{ab} A_a A_b^* , \tag{1}$$

$$a \equiv (J_1 P_1 M_1) ,$$

$$b \equiv (J_2 P_2 M_2) .$$

In this expression the density matrix, ρ_{ab}, is assumed to describe the production of 3π states, averaged (summed) over initial (final) proton

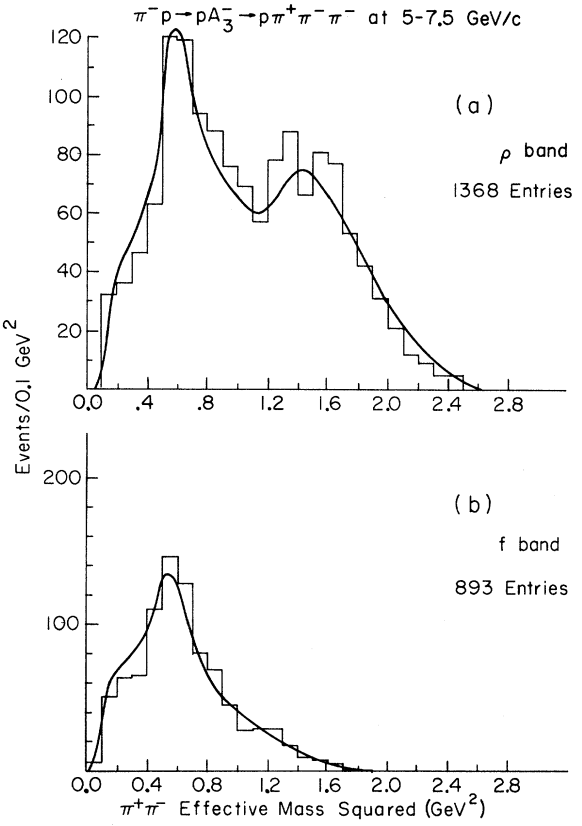

FIG. 9. (a) ρ^0 band (0.665–0.865 GeV); (b) f^0 band (1.14–1.36 GeV) projections for A_3 region of the 5–7.5-GeV/c data (see Ref. 12).

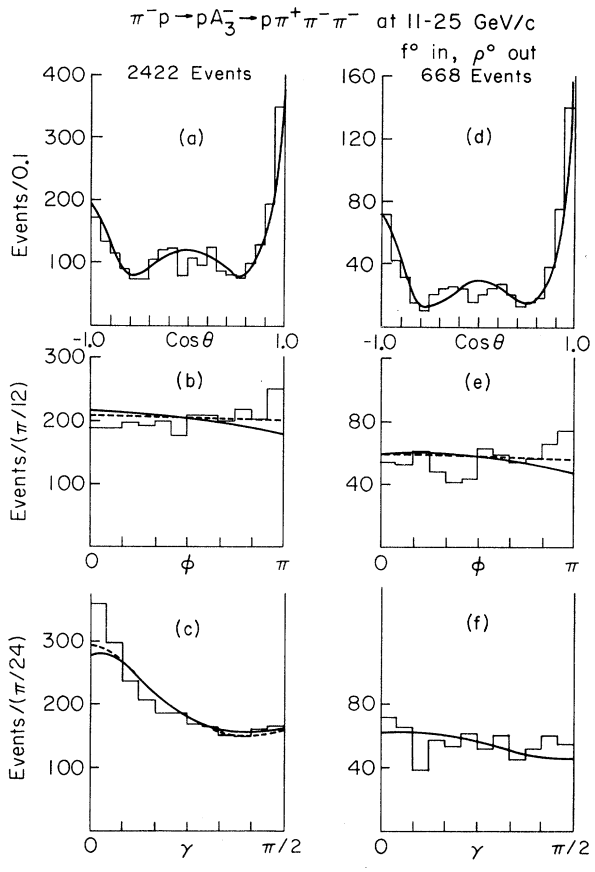

FIG. 10. Euler-angle distributions (Gottfried-Jackson frame) for the A_3 region of the 11–25-GeV/c data (see Ref. 12). (a)–(c) refer to all events in the A_3 region; (d)–(f) refer to events in f^0 bands (1.14–1.36 GeV), but not in ρ^0 bands (0.665–0.865 GeV). The Euler angles are defined in the text.

spin variables, and averaged over the other variables $(s, t, M_{3\pi})$ of the data sample. The A's are amplitudes that describe the "decay" of a state into the final 3π configuration. In this paper these decay amplitudes are calculated on the assumption that they are dominated by cascade processes, $A^- \to R^0\pi^- \to (\pi^+\pi^-)\pi^-$, with R^0 one of the well-known $\pi\pi$ resonances. To allow for the possibility of more than one decay mode we expand the decay amplitudes A^{JPM} into a linear superposition of amplitudes, each corresponding to one decay mode:

$$A^{JPM} = \sum C_{lS}^{JP} A_{lS}^{JPM} , \qquad (2)$$

where l is the orbital angular momentum for the $R^0\pi^-$ system, S the spin of R^0. Explicit formulas for the amplitudes A_{lS}^{JPM} are given in Appendix B.

We note that, as written, Eqs. (1) and (2) imply that if more than one decay mode is allowed for some J^P, the resulting amplitudes add coherently. There is no *a priori* reason that this should be so, since in the extreme case that one decay mode arises entirely from a helicity-nonflip production amplitude, another from a helicity-flip amplitude, the two modes would be completely incoherent. The coherence assumption is easily relaxed by treating decay modes with the same $J^P M$ as separate states, each entering separately in the density matrix.

In this paper we have used only dipion resonances with $I = 0, 1$, and $S = 0, 1, 2$. The masses and widths used were

$$S=0: \; M_\epsilon = 0.765 \text{ GeV}, \; \gamma_\epsilon = 0.4 \text{ GeV};$$

$$S=1: \; M_\rho = 0.765 \text{ GeV}, \; \gamma_\rho = 0.135 \text{ GeV};$$

$$S=2: \; M_f = 1.264 \text{ GeV}, \; \gamma_f = 0.15 \text{ GeV}.$$

The values used for the ϵ and ρ were obtained by fitting 3π data in the A_1-A_2 region.[17,18] For the f^0 we used values quoted by the Particle Data Group.[1] The assumption about the $S=0$ π-π phase shift implied by the use of a simple resonance (the ϵ^0) is clearly not correct above the $K\bar{K}$ threshold.[19]

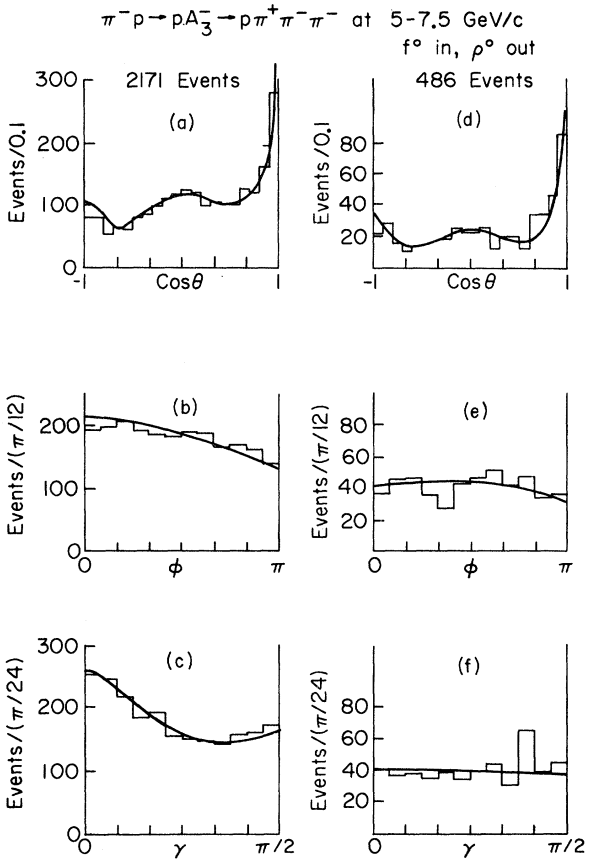

FIG. 11. Euler-angle distributions (Gottfried-Jackson frame) for the A_3 region of the 5–7.5-GeV/c data (see Ref. 12). (a)–(c) refer to all events in the A_3 region; (d)–(f) refer to events in f^0 bands (1.14–1.36 GeV), but not in ρ^0 bands (0.665–0.865 GeV). The Euler angles are defined in the text.

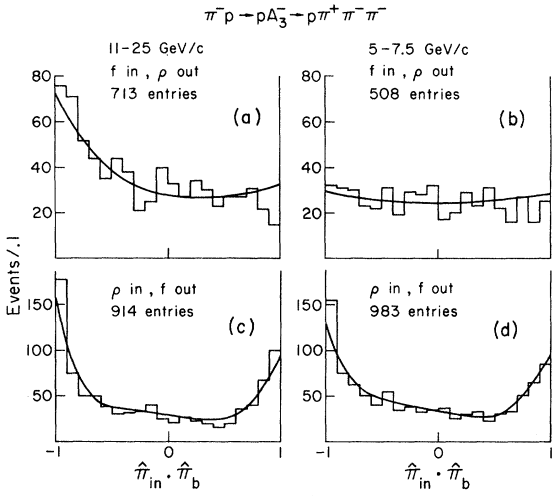

FIG. 12. $\hat{\pi}_{in} \cdot \hat{\pi}_b$ distributions for f^0 and for ρ^0 events: (a) f^0 events, 11–25-GeV/c data; (b) f^0 events, 5–7.5-GeV/c data; (c) ρ^0 events, 11–25-GeV/c data; (d) ρ^0 events, 5–7.5-GeV/c data. f^0 events are defined as A_3-region events (Ref. 12) with $M(\pi^+\pi_a^-)$ in f^0 (1.14–1.36 GeV) and $M(\pi^+\pi_b^-)$ not in ρ^0 (0.665–0.865 GeV). ρ^0 events are similarly defined. Note that for f^0 events $\hat{\pi}_b = -\hat{f}$ and for ρ^0 events $\hat{\pi}_b = -\hat{\rho}$.

Since the behavior of this phase above the $K\overline{K}$ threshold is not well known at present, we have investigated how sensitive our results are to variations in this phase shift by repeating some of the fits with different assumptions about the $\epsilon(S=0)$ dipion propagator (these assumptions are given in detail in Appendix B). We have found that the results reported in this paper are very stable against reasonable changes in the $S=0$ $\pi\pi$ phase shifts.

In the fitting process the parameters which determine the density matrix ρ_{ab} and the complex coupling coefficients C_{lS}^{JP} are varied to maximize the likelihood, Λ,

$$\Lambda = \sum_{\text{events}} \ln P - \int P d\tau \,. \tag{3}$$

The integral of P is limited to those regions of phase space from which events are accepted. In the fitting process due account is taken of the requirements imposed on ρ_{ab} by parity conservation, and of the requirement that ρ_{ab} must be a Hermitian matrix with no negative eigenvalues.

B. Fits to the A_3 Region

It would be nice if we could apply directly the method just described using all possible J^PM states (up to some reasonable maximum value of J) and every possible decay mode. This approach will not work since the number of parameters required would be prohibitively large. We use therefore a more selective approach based in part on the experience gained in fitting the 3π system at lower masses [the A_1 (Ref. 17) and A_2 (Ref. 18) regions] and in part on a careful examination of the experimental decay distributions.

In the A_1-A_2 region it was found that the assumption of coherence (between different decay modes of a given J^P state) is well satisfied experimentally. Since the assumption of coherence reduces greatly the number of parameters required, we made this assumption at the start of our A_3 study, subject to subsequent reexamination. Also in the A_1-A_2 region we observed that all unnatural-parity states ($J^P = 0^-, 1^+, 2^-, \ldots$) were produced almost entirely in the polarization[20] substates $|J^P 0\rangle$, while in the natural-parity series (only $J^P = 2^+$ is actually observed) the dominant substate was ob-

TABLE II. States and decay modes studied in the A_3 ($M_{3\pi}$ = 1.5–1.8 GeV) region. The states and decay modes underlined were retained for the $M_{3\pi}$-dependence study.

J^P	M^{η} [a]	$\epsilon\pi$	$\rho\pi$	$f\pi$
$\underline{0^-}$	$\underline{0^+}$	$\underline{S}$ [b]	$\underline{P}$	D
$\underline{1^+}$	$\underline{0^+1^+1^-}$	$\underline{P}$	$\underline{SD}$	PF
$\underline{2^-}$	$\underline{0^+1^+2^+1^-2^-}$	D	$\underline{PF}$	$\underline{SD}$
$\underline{3^+}$	$\underline{0^+1^+1^-}$	F	$\underline{D}$	$\underline{P}$
$\underline{4^-}$	$\underline{0^+}$		$\underline{F}$	$\underline{D}$
1^-	All		P	D
$\underline{2^+}$	$\underline{1^+0^-}$		$\underline{D}$	$\underline{P}$
$\underline{3^-}$	All		$\underline{F}$	$\underline{D}$
4^+	1^+			F

"Flat" = incoherent-phase-space term

[a] We use states $|J^P M^{\eta}\rangle \propto |J^P M\rangle + \epsilon\eta(-)^M |J^P -M\rangle$, $\epsilon = (-)^{J+1}P$.
[b] The entries S, P, D, F refer to the orbital angular momentum, $l = 0, 1, 2, 3$.

served to be $|J^P 1\rangle + |J^P -1\rangle$. We therefore started with the same assumption about polarizations in the A_3 region, again subject to subsequent reexamination. The assumption that $M = 0$ dominates follows also by looking at the decay angular distributions, which are nearly flat in azimuth (ϕ) but have considerable structure in $\cos\theta$.

In the A_1-A_2 region the most important J^P states and decay modes were found to be $0^-(S \to \epsilon\pi$ and $P \to \rho\pi)$, $1^+(P \to \epsilon\pi$ and $S \to \rho\pi)$, $2^-(P \to \rho\pi)$, and $2^+(D \to \rho\pi)$, with some indications of $3^+(D \to \rho\pi)$. In the A_3 region we expect (and see in the data) the onset of the $f^0\pi$ decay mode, mostly via S wave (only 2^- can contribute) with evidence for some P wave (1^+, 2^+, and 3^+ can contribute to the P wave). After an initial selection of states we studied very carefully the data in the A_3 region ($M_{3\pi}$ = 1.5–1.8 GeV) doing a large number of fits in which a few states at a time (to avoid the need of too many parameters) were added to the initial set.

Table II gives a list of all states and decay modes considered in this study. The more important ones (underlined in the table) were selected for a study of the $M_{3\pi}$ dependence. This set includes all states and decay modes mentioned in the preceding discussion, with the exception of $1^+(P \to f\pi)$, which was found to be negligible. The set also includes a phase-space term (labeled "flat") which gives rise to a uniform distribution in decay space (Dalitz plot + Euler space) and which does not interfere with any other terms. This term was included to explore the possible occurrence of a direct 3π decay mode in spite of the fact that no need for it was found in any of our fits. Most of the remaining states and decay modes (those not underlined in Table II) were completely rejected by the fits or resulted in completely negligible contributions ($\lesssim$1–2% of the events). A few states gave marginally significant contributions in the A_3 region but were clearly too small to be included in fitting the smaller data samples available to study the $M_{3\pi}$ dependence. Among these states are $2^-(F \to \rho\pi)$ and $4^-(F \to \rho\pi)$. Also small but finite contributions in the magnetic substates $|J^P 1\rangle - |J^P -1\rangle$ were found for $J^P = 1^+, 2^-, 3^+$. In each case it was found that the results for the remaining states were essentially unchanged by including or omitting these marginal contributions.

How well the fits agree with the data may be judged by looking back at the experimental distributions (Figs. 6–12). In the figures the solid lines correspond to the fits obtained using only the states and decay modes shown underlined in Table II. The agreement is satisfactory with significant discrepancies only in the azimuthal (ϕ) distribution for all events [Fig. 10(b)], in the γ distribution for all events [Fig. 10(c)], and in the $\hat{\pi}_{\text{in}} \cdot \hat{\rho}$ distribution for ρ-π events [Fig. (12)]. The dashed lines (where shown) are the result of fits with the states $|J^P 1\rangle - |J^P -1\rangle$ added for $J^P = 1^+, 2^-$ (but not 3^+) and with $2^-(F \to \rho\pi)$ also added. The γ distribution seems to indicate a need for inclusion of $\rho\pi$ decay modes with higher spins; the addition of a $4^-(F \to \rho\pi)$ term improves the fit somewhat, but even higher spins appear to be required. Since none of these effects are really relevant to our main goal of elucidating the A_3 structure, we have felt it was not worthwhile to push further in the direction of improving the fit to the data.

C. $M_{3\pi}$ Dependence

Having established what states and decay modes are required, we investigated the dependence on the 3π mass by making fits to the data in 0.1-GeV-wide bins from $M_{3\pi}=0.8$ to $M_{3\pi}=2.0$ GeV. The states and decay modes used are those shown underlined in Table II.

The results of the fits to the high-energy data (11–25 GeV) are shown in Figs. 13–17. The fits were made to events with $t'<0.7$ GeV^2. Events with $M(p\pi^+)=1.16$–1.32 GeV were not used in the fits, but the results shown have been corrected for this cut.

Figure 13 shows the contribution of the "flat" term (phase-space), the combined contributions of all $\epsilon^0\pi^-$ decay modes, the combined contributions of all $\rho^0\pi^-$ decay modes, and the combined contributions of all $f^0\pi^-$ decay modes. The only structure in the A_3 region occurs in the $f^0\pi^-$ mode.

Figure 14 shows the contributions (for all decay modes) of each J^P state. The only structure in the A_3 region occurs in the state $J^P=2^-$.

Figures 15–17 show the contributions of individual decay modes to the states $J^P=0^-, 1^+$, and 2^-. The only structure in the A_3 region occurs in the $f^0\pi^-$ (S-wave) decay mode of the state $J^P=2^-$.

We therefore associate the A_3 enhancement in the 3π mass spectrum with the $2^-(S\to f\pi)$ state. To determine the mass and width of the A_3, we have fitted the $2^-(S\to f\pi)$ spectrum to a simple Breit-Wigner shape. No background was used. We obtain a mass of 1.66 ± 0.01 GeV and a width of 0.27 ± 0.06 GeV for the A_3. If a background had been used, the mass and width of the A_3 would depend on the shape of the background.

A completely similar analysis was carried out also for the low-energy data (5–7.5 GeV). The only difference in the analysis is that a wider Δ^{++} cut ($M_{p\pi^+}<1.4$ GeV out) was used, and a cut on Δ^0 ($M_{p\pi^-}=1.16$–1.32 GeV out) was also made. The results were again corrected for these Δ cuts. The results obtained were quite similar to those for the high-energy data, but are somewhat less certain because of the drastic cuts. We present here only the results for the 2^- state (Fig. 18). The main uncertainty caused by the cuts turned out to be in the amount of $2^-(P\to\rho^0\pi)$, the amount found depending on the width of the Δ^0 cut. If no Δ^0 cut at all is made a (marginal) peaking of $2^-(P\to\rho^0\pi)$ in the A_3 region is seen.[21]

We would now like to comment on some other features of the results shown in Figs. 14–17. A large enhancement in the 1^+ state in the A_1 region is observed. Spin-parity 0^- peaks in that region as well. The 2^+ state shows a Breit-Wigner shaped peak around 1.3 GeV corresponding to the A_2.[18] The $0^-(P\to\rho\pi)$ state shows a clear peak in the A_1 region; however, throughout the mass region considered the $0^-(S\to\epsilon\pi)$ state is larger than the $0^-(P\to\rho\pi)$ state. The $1^+(S\to\rho\pi)$ state peaks strongly around 1.1 GeV and is roughly 0.3 GeV wide. This is the state which is normally associated with the A_1.[17] The amount of the $1^+(P\to\epsilon\pi)$ state is approximately constant in the mass region investigated and it exceeds the $1^+(S\to\rho\pi)$ contribution for masses higher than 1.4 GeV.

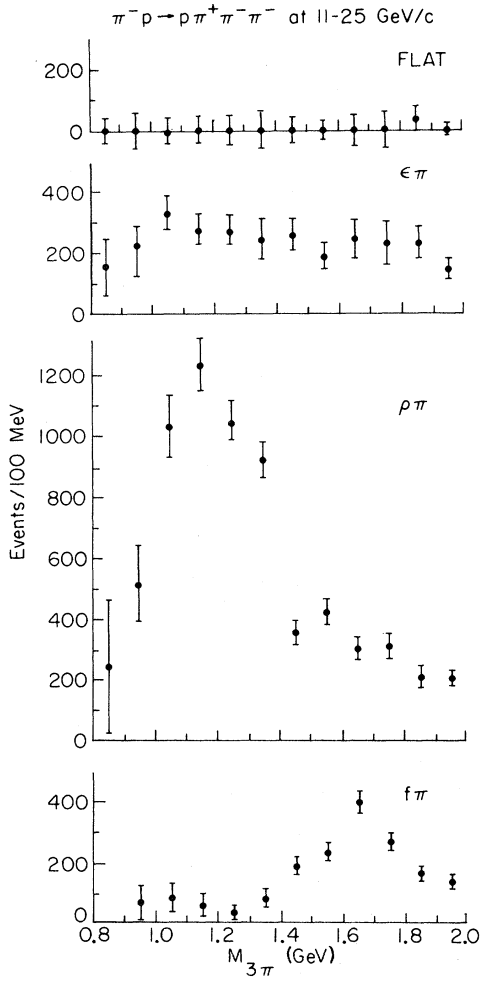

FIG. 13. "Flat," $\epsilon\pi$, $\rho\pi$, and $f\pi$ contributions vs $M_{3\pi}$, 11–25-GeV/c data, $t'<0.7$ GeV^2. "Flat" refers to a term with uniform distribution in Dalitz plot and Euler space.

D. J^P and Branching Ratios of A_3

The results of the fits described in the previous sections are that no structure in the A_3 region is seen except in the state $J^P=2^-$ in the $f^0\pi$ (S-wave) channel. Since no other structure was seen we

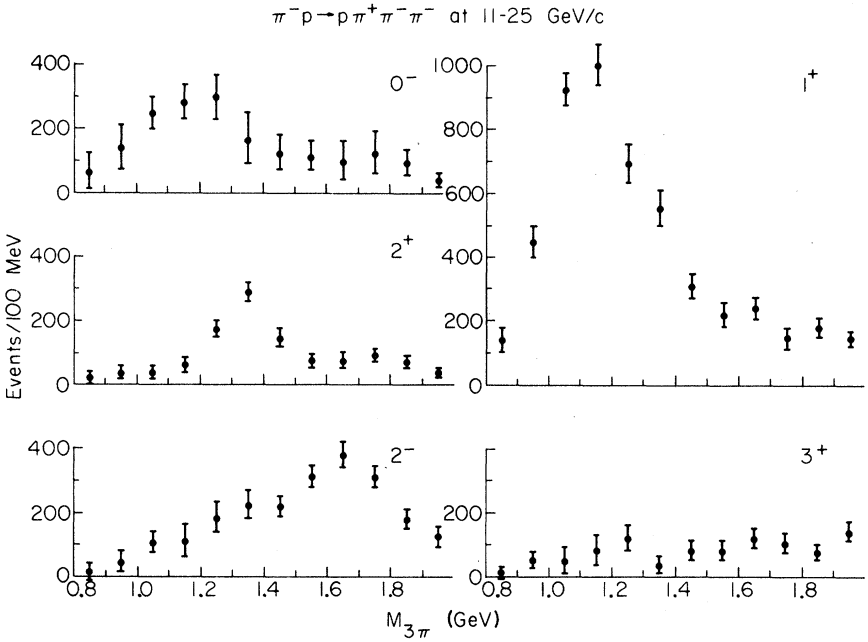

FIG. 14. Contributions of $J^P=0^-$, 1^+, 2^-, 2^+, 3^+ states vs $M_{3\pi}$ for 11–25-GeV/c ($t'<0.7$ GeV^2) data.

can only put upper limits to the contributions of other decay modes of the state $J^P=2^-$ and to the contributions of other J^P states to the A_3 enhancement.

For the states and decay modes which were included in the $M_{3\pi}$-dependence study (underlined in Table II) we can obtain upper limits for the respective contributions to the A_3 effect by drawing a smooth background and by taking into account statistical fluctuations. For the states which were not included in the $M_{3\pi}$-dependence study, but which were studied in the $M_{3\pi}=1.5$–1.8 GeV region (these are shown not underlined in Table II) we can estimate an upper limit by assigning to the A_3 the respective contributions (if any) obtained from fits in $M_{3\pi}=1.5$–1.8 GeV. In this way we arrive, for example, at the following upper limits for alternate decay modes of the 2^- state:

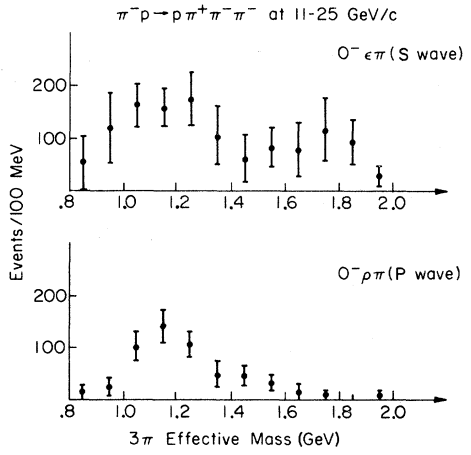

FIG. 15. Contributions of $0^-(S\to\epsilon\pi)$ and $0^-(P\to\rho\pi)$ vs $M_{3\pi}$ for 11–25-GeV/c ($t'<0.7$ GeV^2) data.

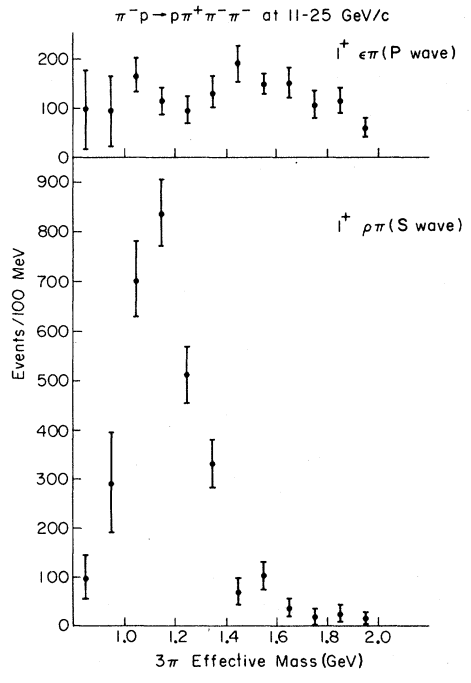

FIG. 16. Contributions of $1^+(S\to\rho\pi)$ and $1^+(P\to\epsilon\pi)$ vs $M_{3\pi}$ for 11–25-GeV/c ($t'<0.7$ GeV^2) data.

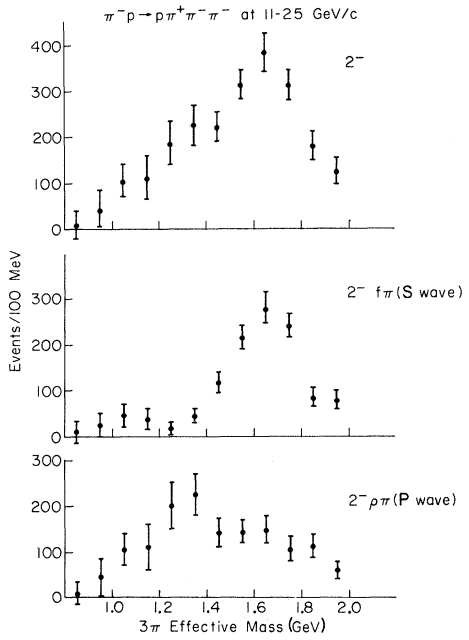

FIG. 17. Total $J^P = 2^-$, $2^-(S \to f\pi)$ and $2^-(P \to \rho\pi)$ contributions vs $M_{3\pi}$ for 11–25-GeV/c ($t' < 0.7$ GeV^2) data.

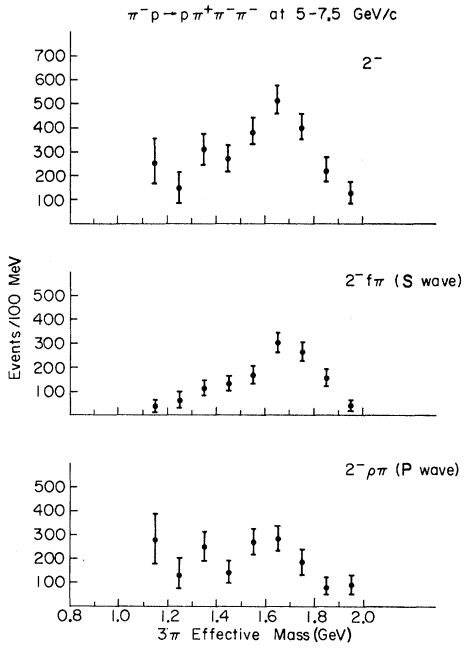

FIG. 18. Total $J^P = 2^-, 2^-(S \to f\pi)$ and $2^-(P \to \rho\pi)$ contributions vs $M_{3\pi}$ for 5–7.5-GeV/c ($t' < 0.7$ GeV^2) data.

$$2^-(P \to \rho^0\pi^- \to \pi^+\pi^-\pi^-) \lesssim 10\% ,$$

$$2^-(D \to \epsilon^0\pi^- \to \pi^+\pi^-\pi^-) \lesssim 6\% ,$$

$$2^-(F \to \rho^0\pi^- \to \pi^+\pi^-\pi^-) \lesssim 10\% ,$$

$$2^-(D \to f^0\pi^- \to \pi^+\pi^-\pi^-) \lesssim 6\% ,$$

where the fractions are all relative to the amount of $2^-(S \to f^0\pi^- \to \pi^+\pi^-\pi^-)$.

With regard to a possible "3π" effect in the A_3 region we remark that in the fits described we found no evidence of structure in the $\epsilon^0\pi$ channel in any J^P state and no evidence of structure (in fact, no contributions at all) in the "flat" term. The "flat" term, in our analysis, corresponds to a term which has not only a uniform distribution over the Dalitz plot but also an isotropic distribution in the decay angles. Furthermore the "flat" term is not allowed to interfere with any other terms. It is conceivable that a term without appreciable Dalitz-plot structure but with a nonisotropic angular distribution could be missed in our fits. To circumvent this possibility we have also made Dalitz-plot fits to the data, i.e., fits which ignore the angular distributions. These fits – described in Appendix A – also show no structure in "3π" in the A_3 region and lead us to conclude that an upper limit of about 20% [relative to $2^-(S \to f^0\pi \to \pi^+\pi^-\pi^-)$] can be placed on the contribution of a 3π term (defined as a term showing no appreciable Dalitz-plot structure) to the A_3 phenomenon.

IV. PHASE OF THE A_3 AMPLITUDE

Our results show that only the $2^-(S \to f\pi)$ contribution peaks in the A_3 region. As previously mentioned, the peak is well fitted by a Breit-Wigner shape with $M_{A_3} = 1.66 \pm 0.01$ GeV and $\Gamma_{A_3} = 0.27 \pm 0.06$ GeV. If the observed peak is due to the $f^0\pi^-$ decay of a $J^P = 2^-$ resonance, the production phase should be $\phi_{A_3} = \phi_0 - \mathrm{Arg}(M_{A_3}^2 - M_{3\pi}^2 - iM_{A_3}\Gamma_{A_3})$. While we cannot observe this phase directly we do obtain from our fits the difference between this phase and the phase of other production amplitudes. Since there is no evidence of structure associated with other production amplitudes it is natural to assume that these other amplitudes do not undergo any rapid variation in phase as we cross the A_3 region. Therefore any rapid change in the phase difference between the $2^-(S \to f^0\pi^-)$ amplitude and one of the other amplitudes may be reasonably expected to reflect corresponding changes in the $2^-(S \to f^0\pi^-)$ phase. Such rapid phase changes should be seen in the A_3 amplitude, as they were seen by a similar analysis of the A_2,[18] if the A_3 is a resonance.

Figure 19(a) shows the difference between the $2^-(S \to f^0\pi^-)$ phase and the $2^-(P \to \rho^0\pi^-)$ phase, as a function of $M_{3\pi}$. The phases (in each $M_{3\pi}$ bin)

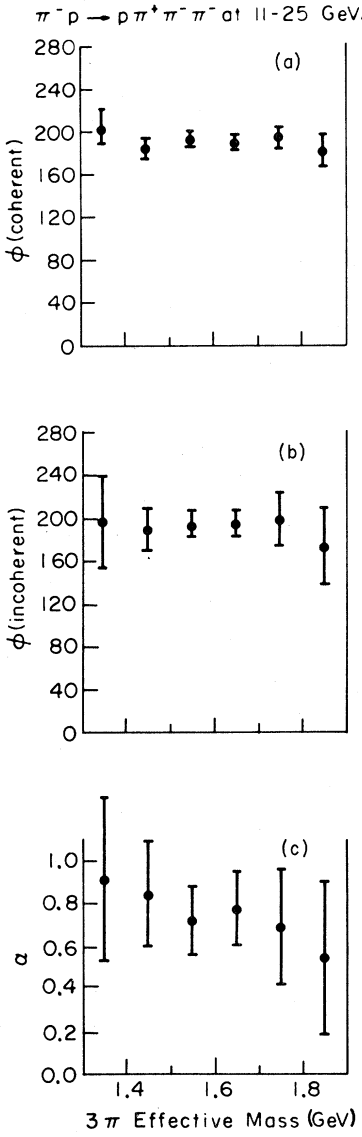

FIG. 19. Phase in degrees of $2^-(S \to f\pi)$ amplitude relative to phase of $2^-(P \to \rho\pi)$ amplitude vs $M_{3\pi}$ for 11–25-GeV/c ($t' < 0.7$ GeV^2) data: (a) $\phi(2^-S) - \phi(2^-P)$ with assumption that 2^-S and 2^-P amplitudes are coherent; (b) $\phi(2^-S) - \phi(2^-P)$ without the coherence assumption; (c) coherence factor, phases are in degrees.

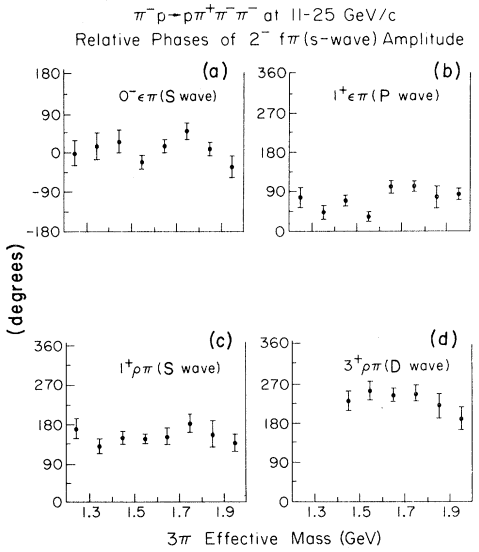

FIG. 20. Phase in degrees of $2^-(S \to f\pi)$ amplitude relative to other amplitudes as a function of 3π mass for the high-energy data. The reference amplitudes are: (a) $0^-(S \to \epsilon\pi)$, (b) $1^+(P \to \epsilon\pi)$, (c) $1^+(S \to \rho\pi)$, (d) $3^+(D \to \rho\pi)$.

are from the result of the fits described in Sec. III C. For each bin the phase is given by $\mathrm{Arg}(C^{2^-}_{Sf^0}/C^{2^-}_{P\rho^0})$; see Eq. (2). There is no sign of any change in this relative phase. The results shown were obtained using the assumption of coherence between amplitudes for different decay modes of the same J^P state. In particular the $2^-(S \to f^0\pi^-)$ and $2^-(P \to \rho^0\pi^-)$ amplitudes were assumed to be coherent. To test this assumption, we have repeated the $M_{3\pi}$-dependence study without the coherence assumption. This means that $2^-(S \to f^0\pi^-)$ and $2^-(P \to \rho^0\pi^-)$ enter separately in the density matrix. In this case the relative phase $\phi(2^-S) - \phi(2^-P)$ is given by the phase of the interference matrix elements ρ_{SP} (we abbreviate 2^-S to S and 2^-P to P). The degree of coherence is given by $\alpha = |\rho_{SP}|/(\rho_{SS}\rho_{PP})^{1/2}$. The coherence assumption corresponds to forcing α to have its maximum value $\alpha = 1$. The results of these fits are, within errors, the same as those obtained previously. Figure 19(b) shows the relative phases $\phi(2^-S) - \phi(2^-P)$ obtained in these fits and Fig. 19(c) shows the quantity α. From Fig. 19(c) one can see that, within rather large errors, the hypothesis of coherence is fairly well satisfied. More importantly, one sees that the results for the relative phases are the same (although the statistical errors are larger).

Figure 20 shows the phase of the 2^-S amplitude relative to several other amplitudes [$0^-(S \to \epsilon\pi)$, $1^+(P \to \epsilon\pi)$, $1^+(S \to \rho\pi)$, $3^+(D \to \rho\pi)$]. In all instances the relative phases appear to be – within errors – independent of $M_{3\pi}$. Although the statistical errors are appreciable, it is evident that in no case is the phase variation consistent with the assumption that all of the A_3 bump (or a substantial part of it) is due to the decay of a resonance.

V. t DEPENDENCE AND POLARIZATION OF THE A_3

Figure 21 shows the momentum-transfer dependence of the $2^-(S \to f\pi)$ contribution to the data in the $M_{3\pi} = 1.5$–1.8-GeV interval. The results

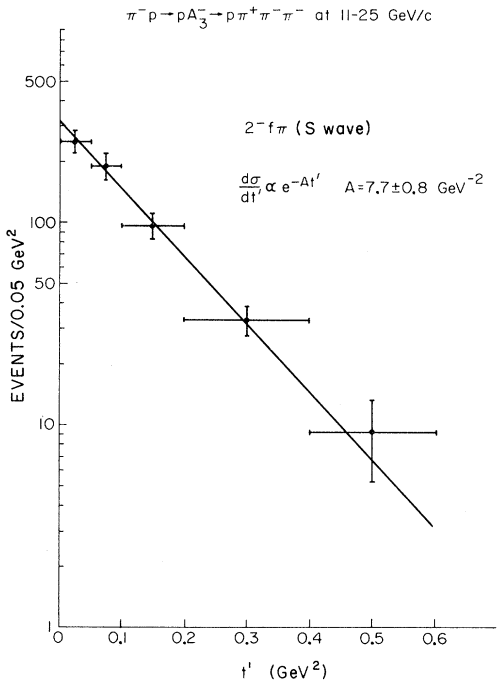

FIG. 21. Number of $2^-(S \to f\pi)$ events in $M_{3\pi} = 1.5$–1.8 GeV vs t', for 11–25-GeV/c data.

refer to the combined results of the high-energy experiments ($p_{\text{lab}} = 11$–25 GeV/c, $\bar{p}_{\text{lab}} \sim 17$ GeV/c). The distribution is well fitted by an exponential dependence on t'. A fit of the form $d\sigma/dt' \propto \exp(-At')$ gives a slope $A = 7.7 \pm 0.8$ GeV^{-2}. This dependence is not very different from that for all events in $M_{3\pi} = 1.5$–1.8 GeV, which also shows an exponential dependence on t' with exponent 6.6 ± 0.2 GeV^{-2}.

We have also looked at the polarization of the A_3 (more precisely we have looked at the polarization of the state 2^-) both for all events (in $M_{3\pi} = 1.5$–1.8 GeV) with $t' < 0.7$ GeV^2, and separately in smaller t' intervals. The complete results are shown in Table III. The results may be summarized as follows:

(a) In the t-channel (Gottfried-Jackson) frame the 2^- state is produced dominantly in the substate $|2^-0\rangle$, with a small but measurable contribution in the substate $|2^-1^+\rangle = (|2^-1\rangle - |2^-{-1}\rangle)/\sqrt{2}$. The contributions from the states with $M = \pm 1$ show up in the data mainly through their interference with the $|2^-0\rangle$ state (and with the other $|J^P 0\rangle$ states). We have verified that the results are the same whether or not the state $|1^+1^+\rangle$ is included in the fits.

(b) Within errors, the polarization in the t-channel frame is independent of t'. In particular the statement holds for $\mathrm{Re}(\rho_{01})$, the only density matrix element besides ρ_{00} which is reasonably well determined in our data.

(c) Figure 22 shows the polar-angle distribution of the π^+, both in the t-channel and in the s-channel[14] frames. It is clear from the data that the angular distribution is independent of t' in the t-channel frame but not in the s-channel frame.

TABLE III. A_3 density-matrix elements.

ρ_{mn} \ t' (GeV^2)	t channel 0–0.05	0.05–0.1	0.1–0.2	0.2–0.4	0.4–0.6[a]	0–0.7	s channel 0–0.7
ρ_{00}	0.96±0.11	0.96±0.12	0.91±0.11	0.81±0.12	0.62±0.24	0.94±0.05	0.41±0.04
ρ_{11}	0.01±0.05	0.01±0.06	0.04±0.05	0.07±0.05	0.19±0.12	0.02±0.02	0.25±0.02
ρ_{22}	0.01±0.06	0.01±0.06	0.01±0.06	0.03±0.06		0.00±0.03	0.04±0.02
ρ_{1-1}	−0.01±0.05	−0.01±0.05	−0.03±0.06	−0.06±0.05	−0.14±0.15	−0.01±0.02	−0.25±0.02
ρ_{2-2}	0.00±0.04	0.01±0.05	0.01±0.05	0.03±0.05		0.00±0.02	0.04±0.02
$\mathrm{Re}\rho_{10}$	0.08±0.05	0.09±0.04	0.12±0.05	0.12±0.05	0.14±0.14	0.11±0.02	0.28±0.02
$\mathrm{Im}\rho_{10}$	−0.05±0.14	0.05±0.15	−0.03±0.16	0.03±0.16	−0.01±0.52	−0.01±0.06	−0.01±0.05
$\mathrm{Re}\rho_{20}$	−0.03±0.04	0.03±0.04	−0.03±0.04	−0.05±0.04		−0.03±0.02	0.06±0.01
$\mathrm{Im}\rho_{20}$	0.00±0.15	−0.04±0.13	0.03±0.16	0.00±0.14		−0.01±0.06	0.00±0.06
$\mathrm{Re}\rho_{21}$	−0.01±0.04	0.00±0.03	−0.01±0.04	−0.01±0.04		0.00±0.01	0.09±0.02
$\mathrm{Im}\rho_{21}$	0.00±0.13	−0.01±0.12	0.00±0.13	0.00±0.13		0.00±0.04	0.00±0.04
$\mathrm{Re}\rho_{2-1}$	0.00±0.03	0.00±0.03	0.01±0.03	0.01±0.03		0.00±0.01	−0.09±0.01
$\mathrm{Im}\rho_{2-1}$	0.00±0.15	0.01±0.15	0.00±0.15	0.00±0.18		0.00±0.06	0.00±0.05

[a] ρ_{2n}'s were kept equal to 0 in this fit.

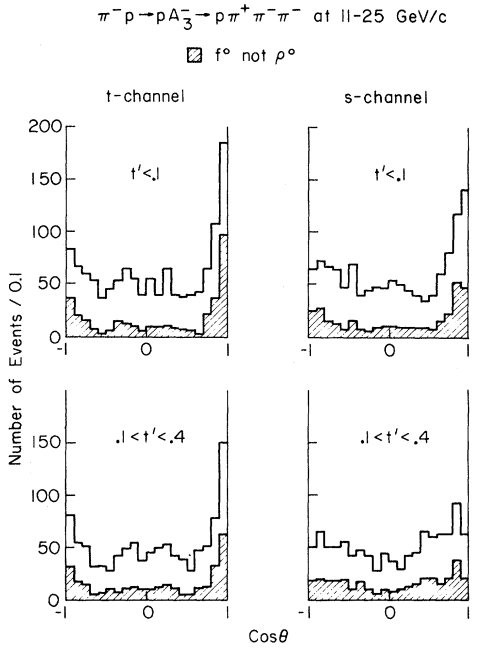

FIG. 22. $\cos\theta$ distributions for events in $M_{3\pi} = 1.5$–1.8 GeV, $M_{p\pi^+} = 1.16$–1.32 GeV out, for 11–25-GeV/c data. Distributions are shown for the t-channel frame ($\cos\theta = \hat{n}_{in} \cdot \hat{\pi}^+$ in 3-π frame) and in the s-channel frame ($\cos\theta = -\hat{p}_{out} \cdot \hat{\pi}^+$ in 3-π frame) for the intervals $t' < 0.1$ GeV^2 and $t' = 0.1$–0.4 GeV^2. The shaded distributions are for events with at least one $\pi^+\pi^-$ mass in the $f^0(1.14$–1.36 GeV) and no $\pi^+\pi^-$ mass in the $\rho^0(0.665$–0.865 GeV).

VI. s DEPENDENCE OF A_3 PRODUCTION

We present for completeness the dependence of the A_3^- production cross section on the incident π^- momentum, although the statistical errors for individual experiments are uncomfortably large and preclude a precise statement about the energy dependence.

TABLE IV. Cross sections.

Momentum (GeV/c)	Cross section (mb) for $\pi^- p \to p\pi^+\pi^-\pi^-$	Number of A_3 events [a]	Cross section (μb) for $\pi^- p \to p A_3^-$ [a]
5	1.76 ± 0.07	366 ± 52	25 ± 4
7	1.83 ± 0.12	135 ± 26	43 ± 9
7.5	1.60 ± 0.10	208 ± 30	31 ± 5
11	1.14 ± 0.10	110 ± 19	37 ± 8
13	1.01 ± 0.09	106 ± 17	50 ± 9
16	1.13 ± 0.05	182 ± 22	39 ± 5
18.5	0.86 ± 0.07	175 ± 23	32 ± 5
20	0.88 ± 0.09	116 ± 17	27 ± 4
25	0.63 ± 0.09	68 ± 20	20 ± 6

[a] The number of A_3^- events and the A_3^- cross section refer only to the $2^-(S \to f^0\pi^- \to \pi^+\pi^-\pi^-)$ contribution in the region $M_{3\pi} = 1.5$–1.8 GeV, and $t' < 0.7$ GeV^2.

The results are shown in Table IV and Fig. 23. We emphasize that we use a narrow definition of the A_3, which includes only the contributions of $2^-(S \to f^0\pi^- \to \pi^+\pi^-\pi^-)$ in the interval $M_{3\pi} = 1.5$–1.8 GeV and with $t' < 0.7$ GeV^2.

The data at 5–7.5 GeV/c include very large corrections for the Δ^{++} and Δ^0 cuts. The data at 11–25 GeV/c are also corrected for the Δ^{++} cut, but the corrections are quite small. We note that above 11 GeV/c the ratio of the A_3 cross section to the cross section for the channel $\pi^- p \to \pi^-\pi^-\pi^+ p$ is – within errors – independent of p_{lab} from 11 to 25 GeV/c. In the same p_{lab} region the data are consistent with a power-law dependence on p_{lab} ($\sigma \propto p_{lab}^{-N}$) with $N = 0.8 \pm 0.3$. The fit is shown in Fig. 23.

VII. CONCLUSION

It has been the aim of this paper to present as complete as possible an account of the experimental facts on the properties of the A_3 and on its production. We expect that similarly detailed accounts of the A_1 and A_2 will be presented soon.[17,18] We believe that an attempt to understand the implications of the results should refer simultaneously to the A_1, A_2, and A_3 data and to their interrelationship. We have in mind in particular the relative phases and the momentum dependence. The lack of phase change for the A_3 amplitude with the 3π mass, the t dependence and s dependence, and the polarization need to be understood, as well as the very similar behavior for the A_1.[17] The lack of phase change for the A_3 disagrees with the assumption that all (or a substantial part) of the A_3 phenomenon can be interpreted as due to the decay of a resonance. The result is, presumably, in agreement with a Deck-mech-

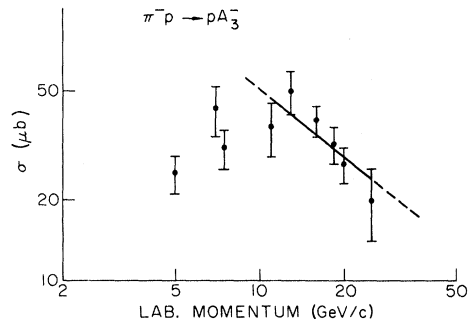

FIG. 23. Cross section for $\pi^- p \to A_3^- p$ vs incident momentum. The cross sections refer only to the production of $\pi^+\pi^-\pi^-$ with $M_{3\pi} = 1.5$–1.8 GeV and $t' < 0.7$ GeV^2 through the amplitude $2^-(S \to f^0\pi^- \to \pi^+\pi^-\pi^-)$.

anism interpretation. We are reluctant however to accept the view that the A_3 (and A_1) phenomena are understood consequences of the Deck hypothesis.

To make this conclusion acceptable, one would need a more realistic and more detailed evaluation of the model, capable of accounting for most, if not all, of the observations in the A_1-A_3 region. Such an evaluation, if successful in giving a coherent interpretation of the data, would also open up the possibility of testing theoretical predictions regarding the phase of the A_2 production amplitude, including its dependence on s and t.

ACKNOWLEDGMENTS

We would like to acknowledge the help of the scanning, measuring, and technical staffs at each of our laboratories. Also we would like to thank the bubble-chamber staffs at Argonne National Laboratory, Brookhaven National Laboratory, CERN, Lawrence Berkeley Laboratory, and Stanford Linear Accelerator Center for providing us with the film.

APPENDIX A: DALITZ-PLOT ANALYSIS

We describe briefly the results obtained when a Dalitz-plot analysis is applied to the high-energy (11–25 GeV/c) data. The event selection is the same as for the analysis of the complete decay distribution (referred to as the "complete" analysis in this appendix); we select events with t' < 0.7 GeV^2 and reject events with $M_{p\pi^+}$ = 1.16–1.32 GeV. No corrections for the $M_{p\pi^+}$ cuts were made, since these require taking into account the polarizations.

Three reasons motivated our Dalitz-plot analysis:

(1) We wanted to compare resolution and results for the two methods.

(2) We wanted to investigate whether apparent inconsistencies between our results and some previously published results of Dalitz-plot analyses are significant.

(3) We wanted to reexamine the question of a possible "3π" decay mode in the A_3 region.

Two sweeps of the data for $M_{3\pi}$ = 1.3–2.0 GeV in 0.1-GeV bins were carried out using two different sets of states. The states used and the results are shown in Figs. 24 and 26(a) for one sweep, and in Figs. 25 and 26(b) for the other.

In the first sweep we used the states included in a published Dalitz-plot analysis of the $\pi^-\pi^+\pi^+$ system produced in the reaction $\pi^+p \to \pi^-\pi^+\pi^+p$ at[7] $p_{\rm lab}$ = 11.7 GeV/c except that $2^+(D \to \rho\pi)$ was re-

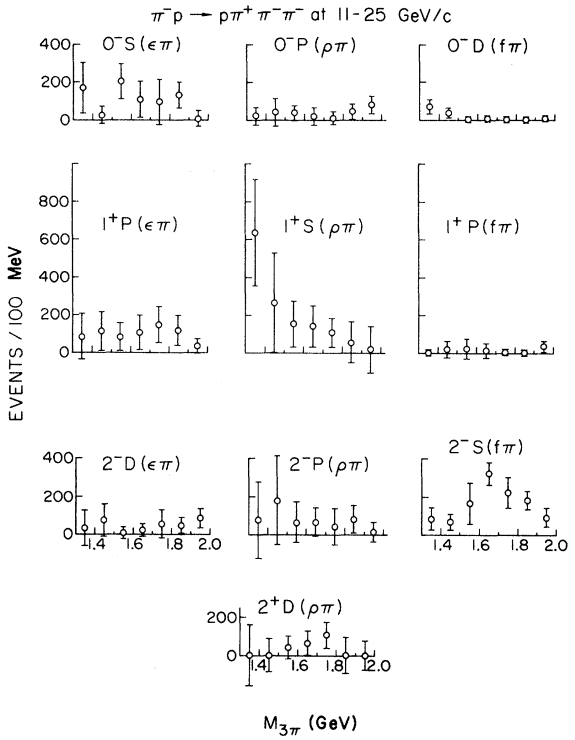

FIG. 24. Results of Dalitz-plot fits to the 11–25-GeV/c data (t' < 0.7 GeV^2, $M_{p\pi^+}$ = 1.16–1.32 GeV out). Only the states and decay modes shown in the figure were included in the fit.

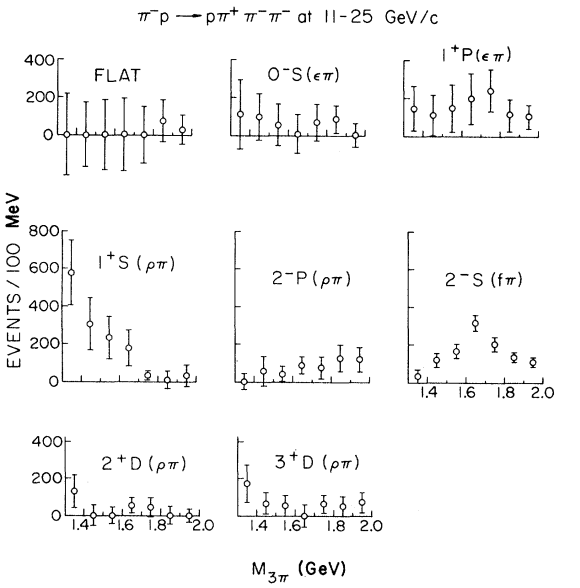

FIG. 25. Results of Dalitz-plot fits to the 11–25-GeV/c data (t' < 0.7 GeV^2, $M_{p\pi^+}$ = 1.16–1.32 GeV out). These fits differ from those in Fig. 24 only in the set of states and decay modes included. "Flat" means a uniform Dalitz-plot distribution.

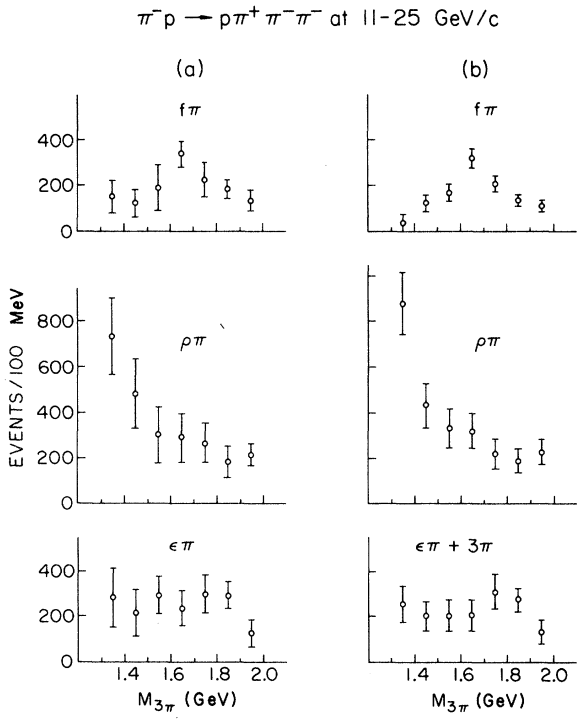

FIG. 26. Results of Dalitz-plot fits, by decay channel: (a) from fits shown in Fig. 24; (b) from fits shown in Fig. 25.

tained. Our results (Fig. 24) should be compared with Fig. 6 of Ref. 7. In the second sweep we wanted to include the same states and decay modes which were used in our "complete" analysis. We experienced some convergence difficulties in doing this, and as a consequence decided to omit $0^-(P \to \rho\pi)$, $2^+(P \to f\pi)$, and $3^+(P \to f\pi)$, which had given relatively minor contributions (above $M_{3\pi} = 1.3$ GeV) in our "complete" analysis. We list our conclusions regarding the results obtained:

(1) The resolution in the Dalitz-plot analyses is substantially worse than in the "complete" analysis. It is particularly difficult, in the Dalitz-plot analysis, to separate within a decay channel (say $\rho\pi$) the contributions of different J^P states. It is also nearly impossible to separate the $\epsilon\pi$ channel from the 3π channel (called "flat" in our figures, and corresponding to a uniform Dalitz-plot population).

(2) The results of our Dalitz-plot analysis of the 11–25-GeV/c π^- data differ in some respects from the results of our "complete" analysis of the same data and from the results of the Dalitz-plot analysis of the 11.7-GeV/c π^+ data reported in Ref. 7. Taking into account the limited resolution of the Dalitz-plot analyses, none of these differences should be considered as significant. We note in particular that neither our Dalitz-plot analysis nor our "complete" analysis confirms the structure in $0^-(S \to \epsilon\pi)$ seen in Fig. 6 of Ref. 7 for the π^+ data.

(3) The results of our Dalitz-plot analyses (Fig. 26) regarding the contributions of the $f\pi$, $\rho\pi$, and $\epsilon\pi + 3\pi$ channels are in excellent agreement with the results of our "complete" analysis. We note that in no case do we see any evidence of structure in the A_3 region in the $\epsilon\pi$ channel, the 3π channel, or the combined $\epsilon\pi + 3\pi$ channel.

APPENDIX B: FORMULAS FOR DECAY AMPLITUDES

We write the amplitude A_{lS}^{JPM} for the decay of a state with spin-parity J^P, $J_z = M$, into the final $\pi_1^-\pi_2^-\pi^+$ state via a dipion resonance, R, of mass M_R, width Γ_R, spin S, with orbital angular momentum l in the intermediate R-π state, as

$$A_{lS}^{JPM} = N \sum_i \sum_{m\mu} \langle JM \mid lSm\mu \rangle p_i{}^l Y_m^l(\hat{p}_i) B_i q_i{}^S Y_\mu^S(\hat{q}_i) \,. \tag{B1}$$

In (B1), N is a positive normalization factor, $\vec{p}_1$ ($\vec{p}_2$) is the momentum of the dipion $\pi^+\pi_2^-$ ($\pi^+\pi_1^-$) measured in the 3π frame, and $\vec{q}_1$ ($\vec{q}_2$) is the momentum of the π^+ in the dipion frame.

The propagator, B_i, for the dipion resonance is taken, except as noted below, to be

$$B_i = (M_R{}^2 - s_i - iM_R\Gamma_R)^{-1}, \tag{B2}$$

$$\Gamma_R = \gamma_R (q_i/q_0)^{2S+1} (M_R/\sqrt{s_i}) \,. \tag{B3}$$

In (B3), γ_R is the reduced width, s_i is the square of the appropriate $\pi^+\pi^-$ mass, and q_0 the magnitude of $\vec{q}_i$ at $s_i = M_R{}^2$.

As discussed in Sec. III A, we have examined the stability of our results against changes in the assumed behavior of the $S=0$, $I=0$ π-π phase shift above $K\bar{K}$ threshold. Three different parametrizations were tried for the propagators B_i for $S=0$. In all three cases the parametrizations (B2), (B3) were used for $\sqrt{s_i}$ below 0.98 GeV (8 MeV below K^+K^- threshold). Above 0.98 GeV we tried the following three alternatives:

(a) B_i as given in (B2),

(b) $B_i = 0.5\ (-iM_\epsilon\Gamma_\epsilon)^{-1}$,

(c) $B_i = (1 - E_0{}^2/2s_i)(-iM_\epsilon\Gamma_\epsilon)^{-1}$ where $E_0 = 1$ GeV.

Alternative (a) was used in all fits reported explicitly in the paper.

†Work supported in part by the U. S. Atomic Energy Commission and by the National Science Foundation.

*Present address: Los Alamos Scientific Laboratory, Los Alamos, New Mexico 87544.

‡On leave of absence from CERN, Geneva, Switzerland.

§ Present address: Brookhaven National Laboratory, Upton, New York 11973.

‖Present address: Physics Department, Rutgers, The State University, New Brunswick, New Jersey 08903.

**Present address: Cambridge Electron Accelerator, Cambridge, Mass. 02138.

††Present address: Department of Physiology, Yale University, New Haven, Connecticut 06520.

‡‡ Present address: Goddard Space Flight Center, Greenbelt, Maryland.

§§ On leave at Max Planck Institute für Physik und Astrophysik, Munich, Germany.

‖‖ Present address: Bank of America, San Francisco, California.

***Present address: Physics Department, University of Colorado, Boulder, Colorado 80302.

†††Present address: Physics Department, Michigan State University, East Lansing, Michigan 48823.

‡‡‡Present address: Physics Department, Duke University, Durham, North Carolina 27706.

[1]Particle Data Group, Phys. Letters 39B, 1 (1972); C. Y. Chien, *Proceedings of an Informal Meeting on Experimental Meson Spectroscopy, Philadelphia,* edited by C. Baltay and A. H. Rosenfeld (Benjamin, New York, 1968), p. 275.

[2]J. Bartsch *et al.*, Nucl. Phys. B7, 345 (1968).

[3]D. J. Crennell *et al.*, Phys. Rev. Letters 24, 781 (1970).

[4]K. Paler *et al.*, Phys. Rev. Letters 26, 1675 (1971).

[5]W. C. Harrison *et al.*, Phys. Rev. Letters 28, 775 (1972).

[6]R. T. Deck, Phys. Rev. Letters 13, 169 (1964).

[7]C. Caso *et al.*, Nucl. Phys. B36, 349 (1972).

[8]D. V. Brockway, Ph.D. thesis, University of Illinois Report No. COO-1195-197, 1970 (unpublished).

[9]We have used here and elsewhere in this paper the notation $2^-(S \to f\pi)$ to denote the production of a state with $J^P = 2^-$, followed by decay, via S wave ($l = 0$), into $f^0\pi$.

[10]The symbol t' refers to $\Delta_{pp}{}^2 - \Delta_{pp}{}^2$(minimum).

[11]The t' cut was made for convenience in the analysis. In fact very few events with $M_{3\pi} < 2$ GeV are removed by the $t' < 0.7$ GeV^2 cut.

[12]We define A_3 region events as events with $M_{3\pi}$ = 1.5–1.8 GeV, $t' < 0.7$ GeV^2 with the additional Δ cuts: $M(p\pi^+) = 1.16$–1.32 GeV out for the 11–25-GeV/c data; $M(p\pi^+) < 1.4$ GeV and $M(p\pi^-) = 1.16$–1.32 GeV out for the 5–7.5-GeV/c data.

[13]See Fig. 26, Appendix A.

[14]t-channel axes are defined by $\hat{z} = \hat{\pi}_{\text{in}}, \hat{y} \propto \hat{p}_{\text{in}} \times \hat{p}_{\text{out}}$ in 3-π frame. For s-channel axes $\hat{z} = -\hat{p}_{\text{out}}$ is used.

[15]With our choice of Euler angles, reflection in the production plane ($y \to -y$) changes $\phi \to \phi + \pi$, $\gamma \to -\gamma$. Interchange of π_1^-, π_2^- labels changes $\gamma \to \gamma + \pi$.

[16]Because we are near $f^0\pi$ threshold, the angles (ϕ, θ) of the π^+ in the 3-π frame are nearly the same as in the f^0 frame. Consequently the distributions in ϕ and $\cos\theta$ for the f^0 reflect directly the polarization of the f^0.

[17]G. Ascoli *et al.*, Phys. Rev. Letters 26, 929 (1971); G. Ascoli *et al.* (unpublished).

[18]G. Ascoli *et al.*, Phys. Rev. Letters 25, 962 (1970); G. Ascoli *et al.* (unpublished).

[19]J. L. Petersen, Phys. Reports 2C, 165 (1971); S. Flatté *et al.*, Phys. Letters 38B, 232 (1972).

[20]Here and elsewhere in the paper statements about polarization refer to t-channel (Gottfried-Jackson) axes, unless a specific reference to s-channel axes is made.

[21]The results shown on page 42 in *Phenomenology in Particle Physics, 1971,* edited by C. Chiu, G. Fox, and A. J. G. Hey (California Institute of Technology, Pasadena, Calif., 1971) were obtained from a preliminary analysis of the low-energy data (5–7.5 GeV/c) with a narrower (1.16–1.32 GeV) Δ^{++} cut and no Δ^0 cut. It is unfortunate that these earlier results were misleading.